# Multifunctional Intelligent Helmet to Enhanced Safety and Comfort of Laborers in the Mining Industry

Harshal Ambadas Durge[1,*], Vijay Mahadeo Mane[1], Arjun Jaggi[2], Preetish Kakkar[3]

[1]Department of Electronic and Telecommunication Engineering, Vishwakarma Institute of Technology, Pune, India

[2]Sr. Director, Client Partner-Lifesciences and Healthcare, HCLTech, California, United States

[3]Senior Computer Graphics Engineer, Adobe, Washington, United States

Received 14 October 2024; received in revised form 03 January 2025; accepted 07 January 2025

DOI: https://doi.org/10.46604/aiti.2024.14394

## Abstract

This study aims to enhance miner safety through real-time monitoring and emergency responses. To achieve this, a multi-functional mining helmet (MFMH) is designed with location tracking via a global system for mobile communications (GSM) and global positioning system (GPS), hazardous gas detection, lighting, and temperature regulation, along with vibration-based alerts for emergency notification. The helmet is tested in simulated mining environments to assess its performance. The system successfully detected hazardous gases at concentrations of 41.23 ppm, triggered automatic lighting when luminosity dropped below 35 lux, and maintained internal temperatures between 26 ℃ and 27 ℃, demonstrating its effectiveness in safety.

**Keywords:** miner safety, detection, location tracking, communication, emergency alerts

## 1. Introduction

Mining operations rank among the most hazardous industries globally, posing significant risks to miners due to frequent exposure to falls, collisions, and dangerous gases such as methane, carbon monoxide, and hydrogen sulfide. These risks are further exacerbated by challenging underground conditions including extreme temperatures and high noise levels. Excessive noise hinders miners from hearing critical alert signals, delays responses, and increase the likelihood of accidents. Despite advancements in mining management systems and safety protocols, persistent and, to some extent, critical challenges, such as delayed accident reporting and communication breakdowns, continue to impede timely interventions. Moreover, extreme underground temperatures pose significant risks, potentially causing heat-related illnesses or fatalities, such as hyperthermia and heat exhaustion, highlighting the urgent need for proactive safety measures.

Over the years, researchers have developed various intelligent helmet systems aimed at enhancing miner safety. For example, a Zigbee-based helmet proposed by Deokar and Wakode [1] integrated gas sensors, accelerometers, and limit switches to facilitate real-time monitoring and emergency alerts. However, these systems have faced limitations, including sensor durability issues and frequent false alarms. Another study by Mishra et al. [2] integrated alcohol detection, fall detection, and navigation systems into Internet of Things (IoT)-enabled two-wheeler helmets, but challenges such as sensor accuracy and internet connectivity remained. The helmet by Patil et al. [3] incorporated sensors for gas, temperature, humidity, and pulse detection, transmitting alerts via Wi-Fi and Thing-Speak. Nevertheless, its reliability was affected by Wi-Fi connectivity issues and sensor malfunctions.

* Corresponding author. E-mail address: harshaldurge8983@gmail.com

English language proofreader: Chih-Wei Chang

A Zigbee-based coal mine monitoring system presented by Rudrawar et al. [4] detected methane, temperature, and humidity. Despite this, it was limited by Zigbee's range and susceptibility to interference. Cao et al. [5] presented an innovative design utilizing thermoelectric refrigeration with air and water cooling, which addressed high-temperature challenges; however, despite its advantages, scalability concerns hindered its practical application. A multi-functional electronic helmet developed for road safety, featuring a global system for mobile communications (GSM), a global positioning system (GPS), solar mobile charging, rain detection, and temperature regulation (26 to 27 ℃). However, its scalability and environmental durability remain key challenges [6].

Gautam et al. [7] introduced an IoT-based embedded system utilizing sensors and actuators connected to a Raspberry Pi for air pollution monitoring and control. Developed in Python, the system includes a web interface for remote monitoring of gas levels. However, scalability and sensor accuracy in diverse environments remain notable challenges Bhagya Lakshmi et al. [8] propose a smart motorcycle helmet that integrates a radio-frequency (RF)-based control system to prevent bike ignition unless the helmet is worn, along with a alcohol sensor to detect intoxication, signaling with a red light. While effective in improving safety, sensor accuracy and system reliability remain key challenges. Similarly, Khedkar et al. [9] discuss an accident detection system that uses GPS for precise location tracking and immediate alerting of emergency services. The system enhances accident response efficiency but faces limitations in remote areas with weak connectivity.

While these studies mark significant advancements, they fall short of providing a comprehensive solution that integrates real-time location tracking, environmental monitoring, and temperature regulation into a single device. Key gaps include the lack of integration of GPS and GSM technologies for reliable location tracking and communication, as well as inadequate temperature maintenance systems to address the thermal challenges faced by miners.

This study aims to bridge these gaps by designing and evaluating a multi-functional mining helmet (MFMH) that integrates GPS and GSM modules for precise real-time location tracking, automated emergency alert systems, and a robust temperature regulation mechanism. Unlike prior works, the proposed helmet combines critical safety features into a unified platform, addressing the limitations of earlier systems in terms of connectivity, sensor reliability, and scalability. The incorporation of advanced monitoring systems allows for the detection of hazardous gas levels, environmental conditions, and miner health metrics. Simultaneously, vibration-based alerts ensure miners receive timely warnings even in high-noise environments.

Furthermore, this study aims to mitigate key safety risks in mining operations, including falls, collisions, and exposure to hazardous gases, while also addressing the thermal challenges that contribute to heat-related illnesses. Through rigorous testing in simulated mining environments, the study evaluates the helmet's performance in real-time monitoring, hazard detection, and emergency response. The findings demonstrate the effectiveness of the MFMH in improving miner safety, significantly contributing to the field of intelligent safety systems for hazardous environments.

## 2. Proposed System

This section elucidates the structural framework of the helmet, encompassing the arrangement and interconnection of various components. It comprehensively outlines the operation of the helmet's internal system, including sensor mechanisms, data processing pathways, and the operational sequence of the helmet's features. The features of the system are categorized into three main functions: notification alerts, automatic lighting and device control, and internal temperature regulation, as illustrated in Fig. 1. Each function includes specific sub-features, such, as helmet impact, gas detection systems, DC light activation based on luminosity, vibration control through mobile devices, and cooling and warming systems. The subsequent sub-sections provide comprehensive descriptions of the components and functional workflows.

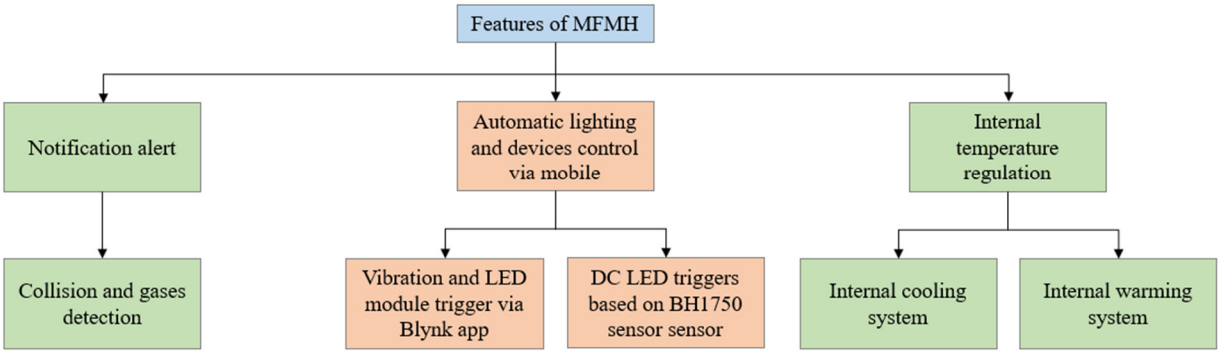


Fig. 1 Features of helmet

### *2.1. Notification alert*

This subsystem is designed to monitor miner safety by detecting collisions, hazardous gases, and the miners' location. This subsystem is comprised of a pancake vibration module, electret microphone, 8-ohm speaker, Neo6M GPS module, SIM800L GSM module, ADXL335 accelerometer, LM2596 regulator, and MQ-2 gas sensor. These components interface with an Arduino Uno microcontroller to generate alert notifications.

The MQ-2 gas sensor detects gas concentrations between 25 to 500 ppm by monitoring resistance changes in its chemi-resistor material. Its heating system, comprising a nickel-chromium coil and aluminum oxide ceramic coated with tin dioxide, facilitates gas detection. Enclosed in dual fine stainless-steel mesh layers for explosion prevention, the sensor's platinum wires with tin dioxide coating respond to current variations. The six-pin configuration includes two heating and four signal pins (A and B), as illustrated in Fig. 2 [6].

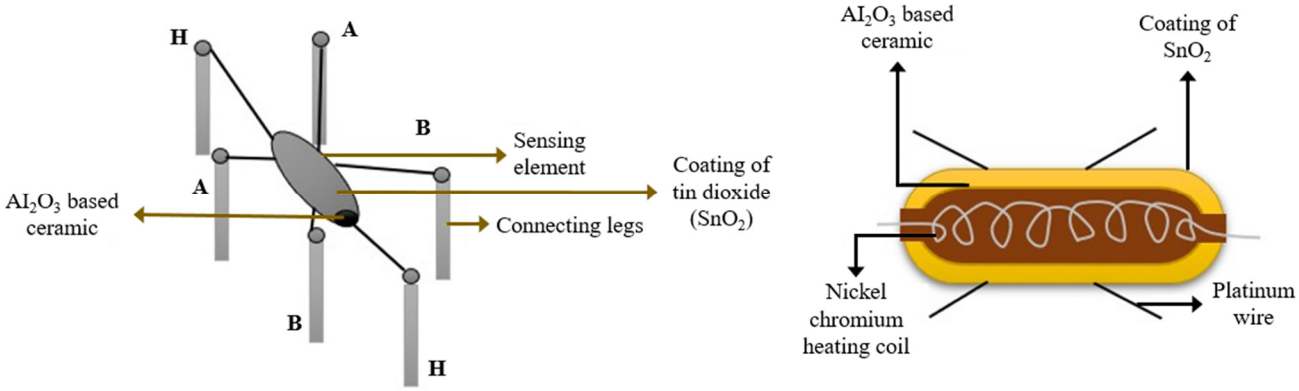


Fig. 2 Internal structure of MQ-3 gas sensor [6]

In clean air, surface oxygen adsorption creates an electron depletion layer in the tin dioxide ($SnO_2$) semiconductor, leading to an increase in resistance. The pressure of gas reduces this adsorption, lowering resistance and allowing electron flow. An LM393 comparator digitizes the analog output for microcontroller processing, triggering a vibration alert when gas levels exceed the threshold [7].

The pancake vibration module operates on piezoelectric technology and eccentric rotating mass (ERM) principles, powered by a 5V supply. It features a flat printed circuit board (PCB) with a three-pole commutation circuit around a central shaft. The system includes a back layer, a base layer, and a front layer, as shown in Fig. 3 [6].

Brushes power the voice coils to create a magnetic field that interacts with a disc magnet, producing flux. During commutation, the magnetic field reverses, activating North-South pole pairs in the neodymium magnet, causing rotation via an off-center mass to generate vibrations. The ERM motor configuration, featuring a six-pole setup, enables simple integration and offers a compact form factor, making it suitable for helmet integration with minimal bulk [8].

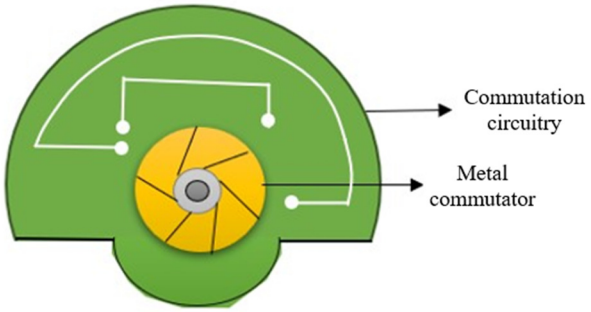


(a) Functional layer (back-side)

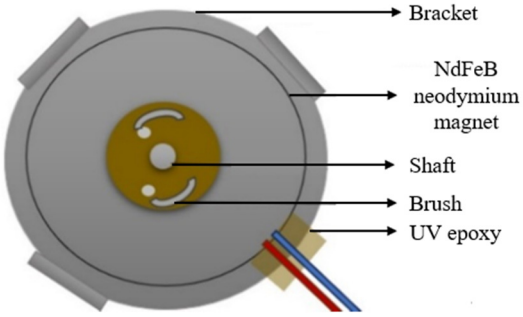


(b) Base-layer

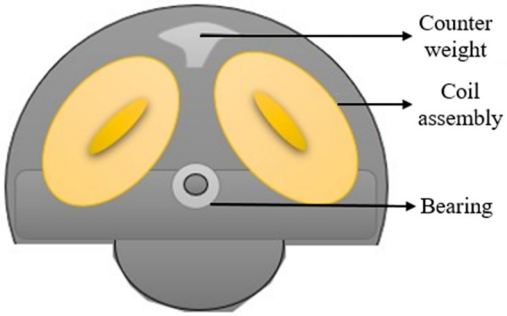


(c) Functional layer (frontside)

Fig. 3 Pancake vibration module [6]

The MQ-2 gas sensor activates a vibration alert upon detecting poisonous gas. Regarding collision scenarios, the ADXL335 accelerometer detects tilt or falls and, using the SIM800L module, sends SMS alerts to emergency contacts. The ADXL335 employs a polysilicon micromachined structure with open-loop acceleration measurement, using polysilicon springs to detect deflection via differential capacitors. Phase-sensitive demodulation determines acceleration magnitude and direction, with bandwidth-regulating capacitors enhancing resolution. Analog outputs for the X, Y, and Z axes are digitized for collision detection based on the following formula [6]. Upon threshold breach, the microcontroller triggers GPS and GSM modules to transmit the miner's location to specified contacts [9].

$$Total_{ACC} = \sqrt{\left(\frac{x_{axis} - 512}{256}\right)^2 + \left(\frac{y_{axis} - 512}{256}\right)^2 + \left(\frac{z_{axis} - 512}{256}\right)^2} \quad (1)$$

The GPS subsystem utilizes the Neo6M module, which receives data from a constellation of 24 satellites orbiting Earth. These signals enable precise location determination, along with velocity, heading, and timing information. Data transmitted in the National Marine Electronics Association (NMEA) format is interpreted by the Arduino IDE through the Software Serial protocol. Each NMEA sentence, prefixed by "$" and an identifier such as "GPGGA", contains essential GPS data including coordinates and accuracy. Parsing this data using specialized functions allows the extraction of location information, such as latitude and longitude [10]

The notification workflow of the MFMH is designed to implement robust real-time safety measures tailored to hazardous mining environments. A critical component of this workflow is the integration of the ADXL335 accelerometer, which can detect abrupt changes in acceleration, tilt, and rotational motion, thereby enabling. The system to identify potential collisions or accidents with high precision. Upon detecting such an event, the accelerometer immediately triggers an alert system that notifies the mining control room. This real-time alert mechanism ensures prompt emergency responses, potentially minimizing the impact of accidents.

Simultaneously, the MQ-2 gas sensor embedded in the helmet operates continuously to monitor the surrounding atmosphere for the presence of dangerous gases, including methane and carbon monoxide. When the detected gas concentrations surpass predefined safety thresholds, the sensor activates a vibration module integrated into the helmet. As a

result, this haptic feedback system delivers direct and immediate warnings to miners, prompting them to evacuate hazardous areas swiftly, and hence minimizing their exposure to toxic gases. Additionally, the system incorporates GPS tracking functionality to render accurate real-time location data. This feature is critical during emergencies, as it enables precise communication of the miner's position to the control room and rescue teams. The GPS data facilitates efficient coordination of rescue operations, significantly reducing response times [11-12].

This comprehensive workflow integrates three key safety features—collision detection, gas exposure warnings, and GPS tracking. Together, these components enhance the overall safety of miners by proactively addressing risks, enabling quicker interventions, and supporting miners in avoiding or mitigating hazardous scenarios. Fig. 4 provides a detailed illustration of the notification workflow implemented within the MFMH system.

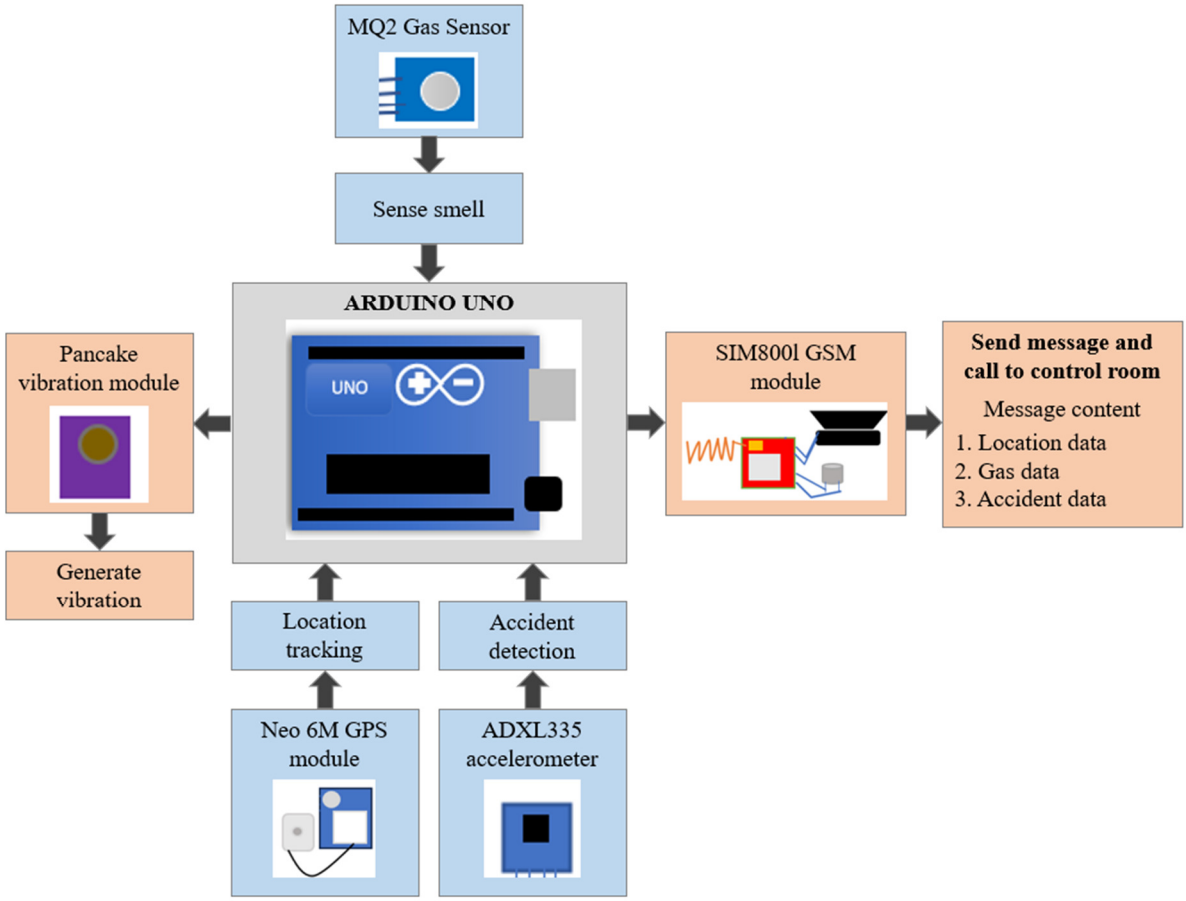


Fig. 4 Notification alert system

### *2.2. Vibration and LED-based emergency alert via the Blynk app and automatic lighting system*

The system is designed to alert workers inside the tunnel through LED lights positioned near the helmet's eye level and vibrations triggered via the Blynk application (Blynk app). Workers operating in low-light environments often need to pause their tasks to manually activate lights; to address this, an automatic lighting system integrated into the helmet activates based on illuminance detected by the BH1750 ambient light sensor.

The system utilizes a Node-MCU, Blynk app, and several hardware components to enable remote alerts for workers. Commands issued through the Blynk mobile app are sent to the Blynk Cloud server and subsequently transmitted to the Node-MCU for processing [13]. During setup, the Node-MCU is configured to interface with vibration modules and the LED light, enabling control of these components based on received commands [14]. In operation, commands from the Blynk app are relayed through the Blynk Cloud server to the Node-MCU [15]. The Node-MCU processes these commands, activating or deactivating the vibration modules and LED light, facilitating effective remote communication [16].

The BH1750 light intensity sensor is employed in this subsystem to measure ambient luminosity [17]. The sensor's photodiode detects incident light, generating electron-hole pairs within the PN junction through the internal photoelectric effect. This process produces an electrical signal proportional to the light intensity, which is then converted into voltage by an integrated operational amplifier (OP-AMP). The system's operating procedure is illustrated in Fig. 5.

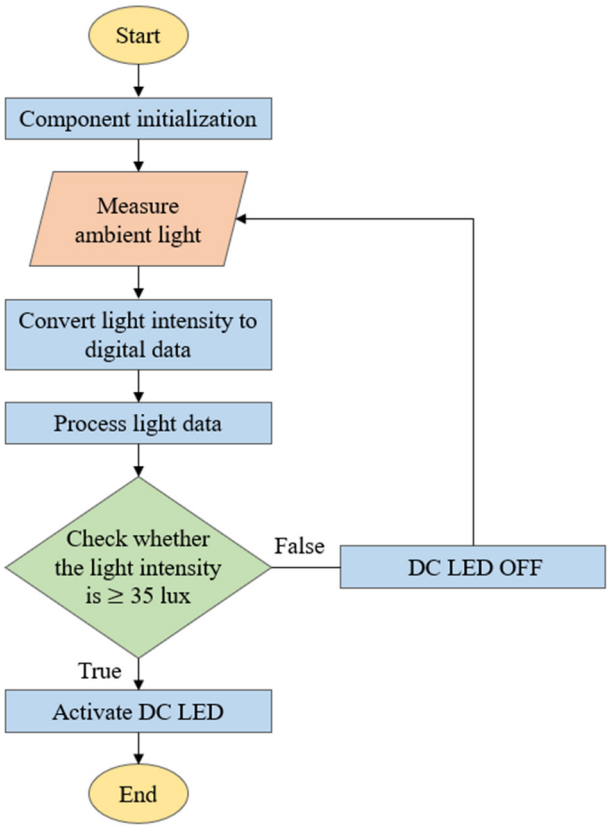


Fig. 5 Automatic DC light system working

The built-in analog-to-digital converter (ADC) converts this voltage into 16-bit digital data representing luminance in lux. The sensor's internal logic unit processes this data and outputs digital lux values via inter-integrated circuit ($I^2C$) communication, with a 320 kHz internal clock oscillator providing the timing reference [18]. When the measured illuminance falls below 35 lux, the relay module's common (COM) terminal connects to the normally open (NO) terminal, activating a DC LED. Conversely, when the lux value exceeds the threshold, the COM terminal connects to the normally closed (NC) terminal, turning off the DC LED [19]. This automated mechanism adjusts lighting based on ambient brightness, ensuring optimal illumination for worker comfort and convenience.

### *2.3. System for internal temperature regulation*

This system comprises a thermostat, LED strip, and power supply designed to regulate the inner surface temperature of the helmet. Utilizing an IP67 Waterproof DimtoWarm LED Light Strip, which adjusts both light intensity and color temperature, the system ensures optimal temperature conditions. The XH-W3001 temperature controller, a digital device known for its precision in temperature control, features programmable capabilities and a relay mechanism for managing power supply to external devices [20]. The controller operates by monitoring the current temperature through an integrated negative temperature coefficient (NTC)-type thermistor, activating or deactivating the connected load as needed.

The XH-W3001 temperature controller features a reset mechanism that activates in the power state by pressing the "up" and "down" buttons simultaneously. Upon reset, the digital display transitions from "888" to the current temperature and restores its settings. The device employs an NTC thermistor as the temperature sensor, which decreases resistance as

temperature increases. If the temperature probe is miscalibrated, the XH-W3001 displays incorrect readings, affecting temperature regulation accuracy. Calibration is indispensable when the displayed temperature deviates from the actual value. This can be corrected using the controller's "temperature offset" feature, which compensates for errors.

The following are the steps to calibrate:

(1) Measure the system's actual temperature using a calibrated sensor.
(2) Compare the actual value to the XH-W3001's displayed reading. If the displayed value is lower, set a positive offset, if higher, set a negative offset.
(3) Adjust the offset by pressing both the "up" and "down" buttons simultaneously to enter offset mode.
(4) Use the "up" or "down" buttons to set the offset value.
(5) Wait for 5 seconds to allow the settings to save.

This process ensures the controller aligns with the actual system temperature for precise regulation. Figs. 6(a) and 6(b) illustrate the hardware connection diagrams for both the cooling and warming features, respectively.

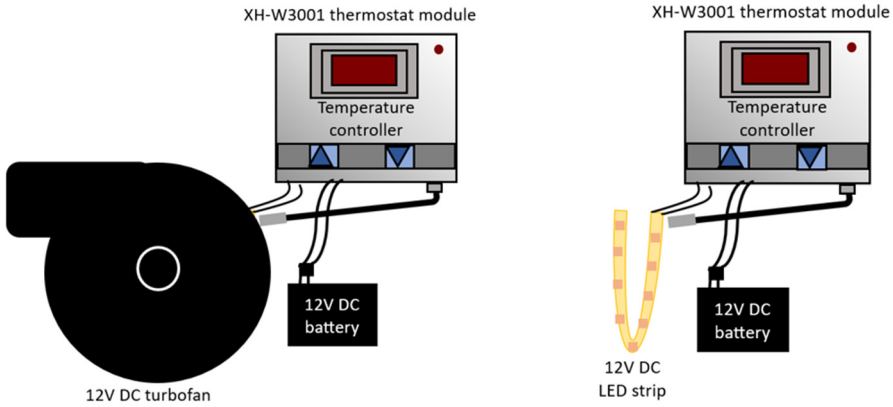


(a) Connection diagram of cooling feature (b) Connection diagram of warming feature

Fig. 6 Temperature regulation hardware interfacing

This feature integrates an internal heating and cooling system to provide comfort to the miner's head within the helmet. The heating mechanism employs a double layer of cotton and foam within the helmet lining for effective heat absorption. Utilizing an XH-W3001 12V DC thermostat, equipped with a built-in relay, the system achieves temperature regulation. The thermostat module, powered by a 12V DC source, controls a 12V DC LED strip and a 12V DC turbofan based on preset conditions. In the warming case, it monitors the current temperature through a 10k NTC thermistor temperature sensor, compares it with predefined temperature settings, and adjusts the relay state accordingly. The LED strip acts as the heat source, converting electrical energy into heat to warm the foam. Configured with start and stop temperatures set at 26 °C and 27 °C, respectively, the system maintains optimal foam temperature. The entire flow of operation is illustrated in Fig. 7.

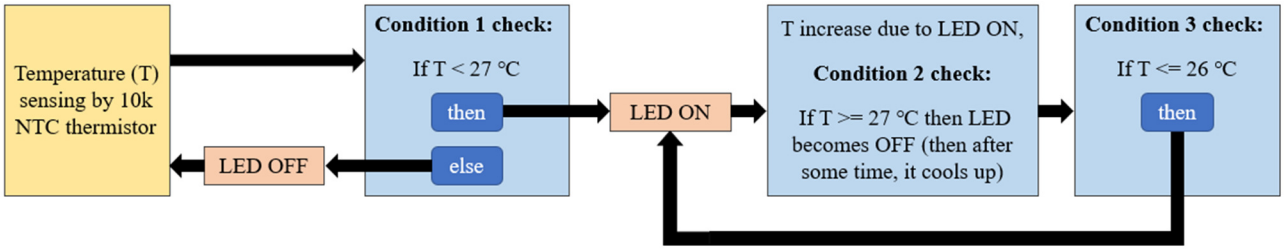


Fig. 7 Workflow of warming feature

During operation, if the ambient temperature initially falls below 27 °C, the thermostat's relay activates, switching on the LED strip to generate warmth. As the foam lining heats up and reaches 27 °C, the relay deactivates to maintain the desired temperature. If the temperature drops back to 26 °C, the relay reactivates to reheat the foam, ensuring consistent warmth [21].

Conversely, when the temperature is relatively high, particularly during summer, the thermostat module operates in cooling mode to alleviate heat discomfort. Initially, when the ambient temperature reaches or exceeds 27 °C, the relay activates, powering a DC cooling fan to generate a stream of cool air. This airflow cools the foam, reducing its temperature. When the temperature drops to or below 26 °C, the relay deactivates, allowing the temperature to rise until it reaches 27 °C. The relay then reactivates to sustain the cooling process. This cyclic process continues until the power supply to the module is terminated, ensuring continuous temperature regulation adapted to seasonal conditions. Fig. 8 provides detailed operational flows, illustrating the complete functionality of the cooling features.

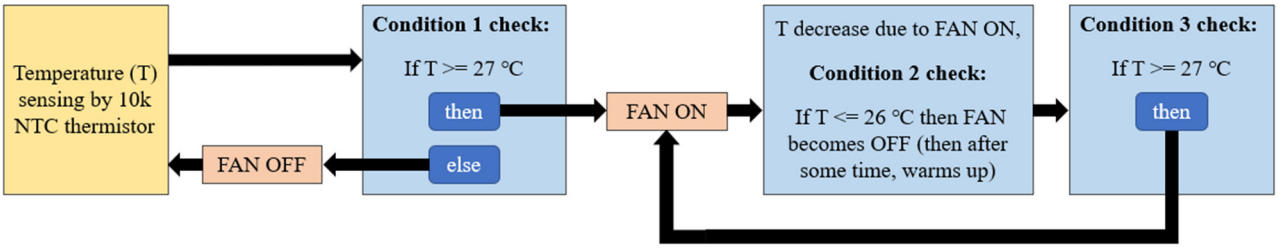


Fig. 8 Workflow of cooling feature

## 3. Results

This section presents the experimental results obtained from testing the model, with a focus on the helmet's temperature regulation, automatic lighting, and notification alert functionalities. The findings encompass interior temperature management, the effectiveness of mobile-controlled vibration and LED indicators, and the overall performance of the notification system.

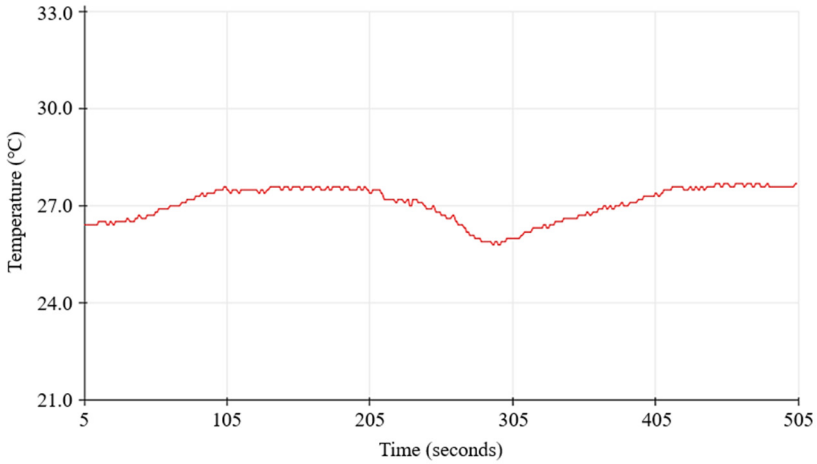


(a) Temperature regulation curve–warming cycle [6]

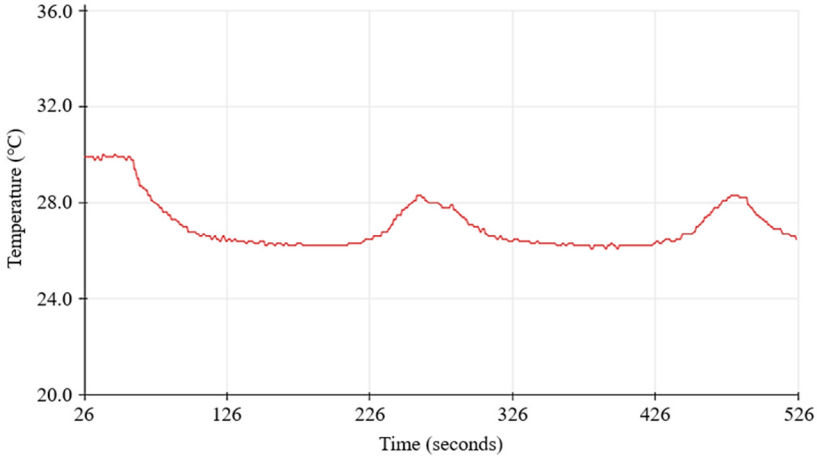


(b) Temperature regulation curve–cooling cycle

Fig. 9 Temperature regulation results

The helmet's warming feature successfully regulated the interior temperature within the specified range of 26 to 27 ℃. Fig. 9 depicts the temperature regulation graph obtained during the testing. The temperature regulation feature effectively maintained the interior temperature within the specified range of 26 to 27 ℃. Figs. 9(a) and 9(b) illustrate the temperature regulation graphs obtained during testing.

In Fig. 9(a), the initial temperature reading was 26.4 ℃, below the maximum threshold of 27 ℃. The LED strip is activated, providing warmth and causing the temperature to rise. Once the maximum threshold was reached, the LED strip was deactivated. The temperature was stabilized for 185 seconds before an observed decrease. The graph shows a decline in temperature until it reaches the minimum threshold of 26 ℃, prompting the LED strip to reactivate. However, the temperature briefly continued to drop to 25.7 ℃ due to sustained external cooling before rising again. This cyclical regulation process persisted [6].

In Fig. 9(b), the initial temperature was 29.6 ℃, exceeding the maximum threshold of 27 ℃. The cooling fan was activated, lowering the temperature. Upon reaching the minimum threshold, the cooling fan deactivated, maintaining the cooler temperature for 120 seconds. Subsequently, a gradual increase in temperature was observed, with the graph showing a rise until the temperature reached the minimum threshold of 27 ℃, triggering the reactivation of the fan. Nonetheless, the temperature continued to rise to 28.1 ℃ before decreasing again due to ongoing external heat, continuing the cyclical process. Figs. 9(a) and 9(b) depict temperature (℃) versus time (seconds) graphs over a total observation period of 500 seconds, ensuring optimal comfort by consistently maintaining the target temperature range.

Fig. 10 presents the vibration signal graph obtained during testing. The x-axis represents time (ranging from 46,075 to 46,575), while the y-axis indicates vibration intensity measured as ADC values (ranging from 352 to 364). The graph illustrates the helmet's vibration intensity over a 5-second interval with the data points recorded every 10 milliseconds. A prominent spike is observed in the graph exceeding an ADC value of 360. This reflects a sudden increase in vibration intensity, caused by an external impact or force acting on the helmet at that moment.

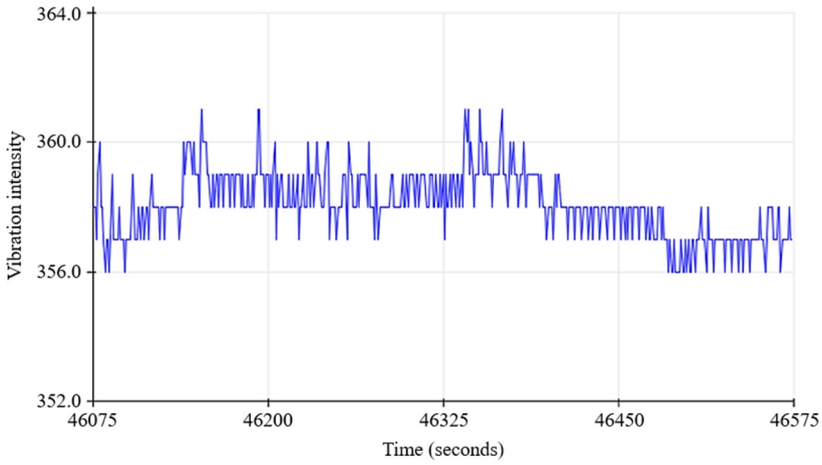


Fig. 10 Vibration signal waveform

The ADXL335 accelerometer sensor detected accidents and visualized the data in the graph, as shown in Fig. 11. This graph presents the resultant acceleration, computed from the combined X, Y, and Z axes accelerometer readings using Eq. (1), plotted over time to illustrate variations in total acceleration. A sudden change in acceleration is evident over a 50-second interval, indicating a potential accident. The x-axis denotes time, spanning from 1966 to 2466 seconds, with each 100 units corresponding to 1 second, while the y-axis represents total acceleration, ranging from −6g to +6g. When the miner fell from a ladder due to a sudden slip, followed by a few seconds of recovery and standing up, the accelerometer measurements recorded during this incident are shown in Fig. 11. The spike in the graph indicates the moment of impact when the helmet hit the ground.

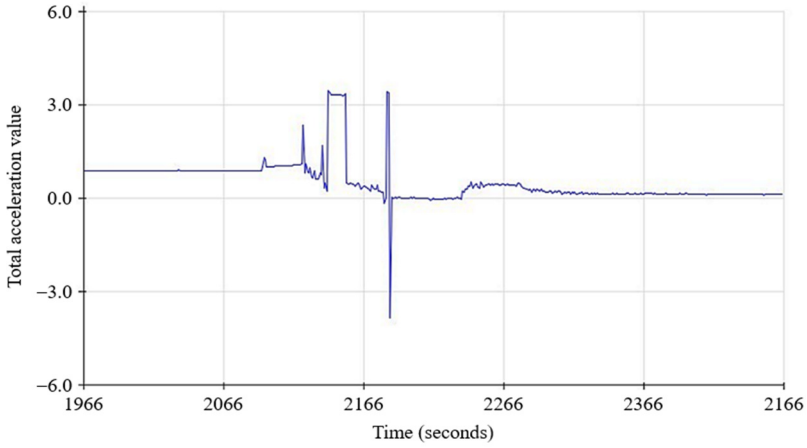


Fig. 11 Accelerometer data graph

Fig. 12 illustrates the graph of gas concentration in parts per million (ppm) detected by the MQ-2 gas sensor worn by a miner over some time. Initially, when the miner first donned the helmet, the gas concentration recorded was 23.45 ppm. Subsequently, when the miner began digging and stopped upon noticing a strange odor, a noticeable spike in gas concentration was observed, reaching 41.23 ppm. This sudden increase is evident in the graph. The data were collected over a total duration of 50 seconds, with measurements taken every 100 milliseconds. The y-axis of the graph represents the gas concentration in ppm, while the x-axis represents time.

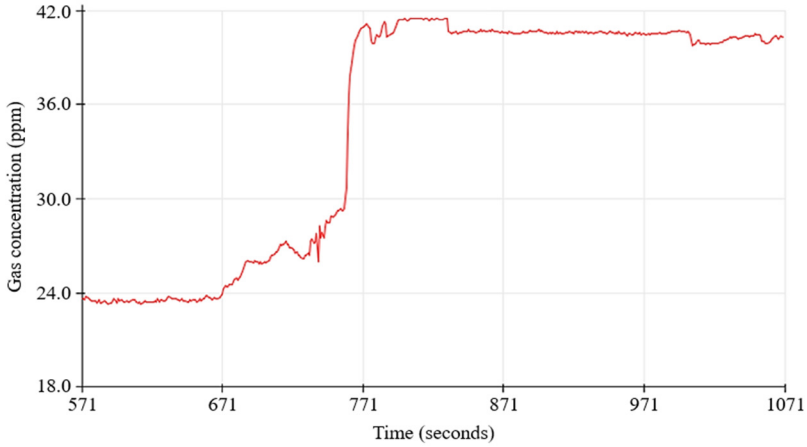


Fig. 12 MQ-2 gas sensor data stream

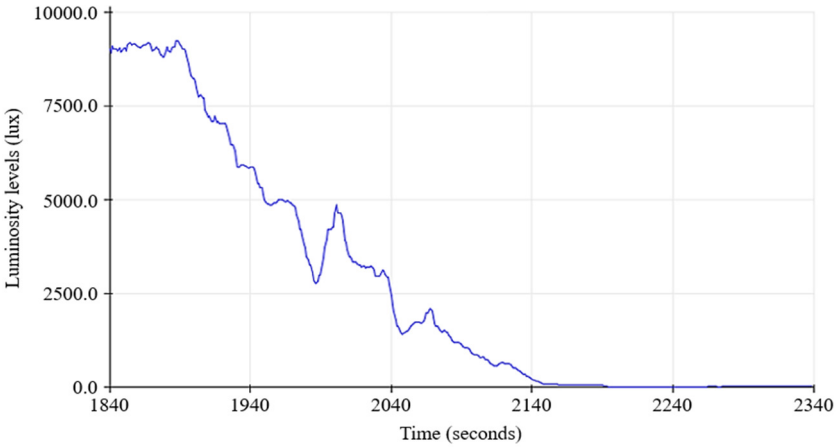


Fig. 13 BH1750 light sensor data stream

The data, as illustrated in Fig. 13, represents the luminosity levels (lux) versus time (seconds) detected by the BH1750 light sensor as a mine worker moves from the entrance to the interior of the tunnel. The graph depicts the variations in luminance encountered during the transition. When the detected luminosity drops below 35 lux, the DC LED light is

automatically activated, ensuring enhanced visibility for the miner without requiring manual intervention. Initially, the sensor recorded 8,992 lux in open sky conditions. As the miner moved deeper into the tunnel, the sensor detected progressively lower light levels, ultimately measuring as low as 10 to 8 lux, as shown in Fig. 13.

The key findings pertinent to the notification system's performance under stringent operational thresholds are summarized in Table 1. The hazardous gases detection system is set to trigger vibration alerts, calls, and messages when gas concentrations exceed 40 ppm, as recommended by mining health experts. Similarly, the accident detection system activates notifications when acceleration surpasses 3 g, as recommended by experts, using data from each axis to detect major injuries. Additionally, the light sensor activates a DC LED based on luminosity levels. Comprehensive data supporting these functionalities are systematically presented in Table 1. These results demonstrate the effective implementation and performance of safety features aimed at enhancing safety and communication reliability for mining workers.

Table 1 Status of notification, vibration alert, and luminosity detection

| Sensor | Observed value | Output (detected) | Triggered response |
|---|---|---|---|
| Accident detection (in g) (Threshold = 3) | | | Message, Call |
| ADXL335 accelerometer sensor | x,y,z: 900,850,950 total acc.: (2.64) | No | OFF |
| | x,y,z: 1000,900,1000 total acc.: (3.09) | Yes | ON |
| | x,y,z: 1100,1000,1100 total acc.: (3.76) | Yes | ON |
| | x,y,z: 950,950,900 total acc.: (2.85) | No | OFF |
| | x,y,z: 540,550,520 total acc.: (0.187) | No | OFF |
| Gas detection (in ppm) (Threshold = 40) | | | Message, Call, Vibration |
| MQ-2 gas sensor | 41.23 | Yes | ON |
| | 21.45 | No | OFF |
| | 52.20 | Yes | ON |
| | 78.80 | Yes | ON |
| | 188 | Yes | ON |
| Luminosity detection (in lux) (Threshold = 35) | | | Relay–LED |
| BH1750 light intensity sensor | 6 | Yes | ON |
| | 11 | Yes | ON |
| | 43 | No | OFF |
| | 10,943 | No | OFF |
| | 30,768 | No | OFF |

The notification feature demonstrated robust performance in warning users of hazardous conditions through vibration alerts, messages, and calls. The vibration signals, as shown in Fig. 10, revealed a significant spike in intensity upon external impact, effectively indicating the precise moment of helmet collision. The accelerometer data, as depicted in Fig. 11, captured sudden acceleration changes exceeding 3 g, visualized as prominent spikes across the X, Y, and Z axes within a 50-second interval, thereby identifying potential high-impact events. The gas concentration, as shown in Fig. 12, was monitored using the MQ-2 sensor, which detected hazardous gas levels exceeding 40 ppm, triggering immediate vibration alerts and notifications. Additionally, luminosity levels, as displayed in Fig. 13, were assessed by the light sensor, which automatically activated LEDs when ambient light dropped below 35 lux, ensuring enhanced visibility in low-light environments.

The next-generation safety helmet redefines protective gear for miners by integrating advanced technologies that enhance comfort, safety, and real-time hazard response. Key features of this innovative design include enhanced temperature regulation and integrated safety systems.

**(1) Enhanced temperature regulation**

- Advancement: Unlike earlier designs that lacked precise thermal control, this helmet maintains interior temperatures within a stringent range of 26 to 27 ℃, ensuring miner comfort and operational consistency.
- Validation: The system's dynamic activation and deactivation of warming and cooling components effectively stabilize temperatures while optimizing energy efficiency, as demonstrated by the temperature regulation graphs in Figs. 9(a) and 9(b).

**(2) Integrated safety features**

- Advancement: Traditional helmets are typically equipped with isolated functionalities, such as gas detection or impact resistance. In contrast, this helmet consolidates multiple safety systems, including hazardous gas alerts, accident detection, automatic lighting, and temperature regulation into a unified device.
- Validation: The system's ability to detect and respond to hazardous gas concentrations exceeding 40 ppm, acceleration levels above 3 g, and luminosity below 35 lux outperforms earlier standalone devices, as evidenced by Table 1 and Figs. 11-13.

**(3) Practical challenges**

Durability

- Challenge: Ensuring resilience against harsh mining conditions, such as high humidity, dust, and mechanical impacts.
- Mitigation: Utilizing durable materials and protective enclosures for electronic components enhances reliability, albeit potentially increasing device weight.

Cost

- Challenge: The integration of advanced sensors and communication modules may elevate production costs, compromising affordability for smaller mining operations.
- Mitigation: Economies of scale through mass production and sourcing cost-effective components are essential to achieving cost efficiency.

Scalability

- Challenge: Adapting the helmet design to diverse mining environments and regulatory requirements may require additional customization.
- Mitigation: Employing a modular design enables seamless upgrades and component replacements, facilitating adaptability across various applications without extensive redesign.

Overall, this next-generation helmet sets a new benchmark in mining safety by combining advanced features with practical design, addressing key challenges while ensuring enhanced protection and operational efficiency.

## 4. Conclusions

This study developed and rigorously evaluated an MFMH designed to address critical safety challenges in mining operations. The helmet integrates advanced technologies, such as GSM and GPS modules for real-time location tracking, accident detection systems, hazardous gas monitoring, internal temperature regulation, and automatic lighting. Extensive testing in simulated mining environments confirmed the helmet's effectiveness in delivering real-time emergency alerts to designated authorities, facilitating prompt responses, and ensuring accurate personnel tracking. The findings underscore the MFMH's significant potential to enhance miner safety by providing essential features that address pervasive risks in mining operations. The hazardous gas monitoring system demonstrated reliable detection of dangerous gas concentrations, while the internal temperature regulation and automatic lighting ensured optimal comfort and visibility under challenging conditions.

To advance practical adoption, this study highlights the need for collaboration with mining organizations and regulatory bodies to develop standardized guidelines mandating the use of such helmets in high-risk operations. Partnering with industry stakeholders to conduct large-scale pilot programs in diverse mining settings can validate the helmet's performance in real-world scenarios, optimize its design for field conditions, and quantify its impact on safety outcomes. Additionally, cost-reduction strategies, such as scalable production and modular design, can make the MFMH more accessible to mining companies of varying capacities. By addressing these factors, this innovative solution can significantly contribute to reducing fatalities and injuries in hazardous mining environments.

## Conflicts of Interest

The authors declare no conflict of interest.

## References

[1] S. R. Deokar and J. S. Wakode, "Coal Mine Safety Monitoring and Alerting System," International Research Journal of Engineering and Technology, vol. 04, no. 03, pp. 2146-2149, 2017.

[2] P. Mishra, P. Pai, P. Singh, V. Kayande, and M. Parmar, "Implementation of a Smart Helmet with Alcohol and Fall Detection and Navigation System," International Conference on Innovative Computing and Communications, vol. 2, pp. 239-251, 2022.

[3] P. J. Patil, M. Bhole, D. N. Pawar, S. Nadgaundi, R. Pawar, and A. Mhatre, "Smart Helmet for Coal Mine Workers," International Conference on Integration of Computational Intelligent System, pp. 1-5, 2023.

[4] M. Rudrawar, S. Sharma, M. Thakur, and V. Kadam, "Coal Mine Safety Monitoring and Alerting System with Smart Helmet," ITM Web of Conferences, vol. 44, article no. 01005, 2022.

[5] L. Cao, J. Han, L. Duan, and C. Huo, "Design and Experiment Study of a New Thermoelectric Cooling Helmet," Procedia Engineering, vol. 205, pp. 1426-1432, 2017.

[6] V. M. Mane and H. A. Durge, "Multifeatured Electronic Helmet to Enhance Road Safety and Rider's Comfort," Proceedings Engineering and Technology Innovation, vol. 28, pp. 41-54, 2024.

[7] A. Gautam, G. Verma, S. Qamar, and S. Shekhar, "Vehicle Pollution Monitoring, Control, and Challan System Using MQ2 Sensor Based on Internet of Things," Wireless Personal Communications, vol. 116, no. 2, pp. 1071-1085, 2021.

[8] A. Bhagya Lakshmi, C. Ragunath, R. Yeswanth, and M. Rajkumar, "Smart Helmet for Riders to Avoid Accidents Using IoT," 2nd International Conference on Computer, Communication and Control, pp. 1-4, 2024.

[9] K. Khedkar, K. Pawar, S. Dhumal, and R. Tandalekar, "Accident Detection and Alert System," International Journal of Scientific Research in Engineering and Management, vol. 8, no. 4, article no. 31371, 2024.

[10] K. Y. Koo, D. Hester, and S. Kim, "Time Synchronization for Wireless Sensors Using Low-Cost GPS Module and Arduino," Frontiers in Built Environment, vol. 4, article no. 82, 2019.

[11] P. Mohare, S. N. Bhatlawande, P. J. Shelke, and K. R. Savalekar, "IoT-Based Accident Detection and Alert System," International Journal of Advanced Research in Science, Communication and Technology, vol. 4, no. 1, pp. 145-148, 2024.

[12] S. Adhav and D. B. Salunke, "Design and Construction of Hazardous Gas Detection and Control System for Electric Vehicle Cabin," International Journal for Research in Applied Science & Engineering Technology, vol. 11, no. VI, pp. 2601-2611, 2023.

[13] N. binti Mazalan, J. K. Elektrik, and P. Merlimau, "Application of Wireless Internet in Networking Using NodeMCU and Blynk App," Seminar LIS at Politeknik Mersing Johor, pp. 1-8, 2019.

[14] Venkateshappa, H. Chethan, C. L. Jayaraj, V. N. Jatinjayasimha, and D. S. Srihari, "Home Automation with Blynk and NodeMCU," Turkish Journal of Computer and Mathematics Education, vol. 12, no. 12, pp. 2669-2674, 2021.

[15] E. Media's, Syufrijal, and M. Rif'an, "Internet of Things (IoT): Blynk Framework for Smart Home," KnE Social Sciences, vol. 8, no. 12, pp. 579-586, 2019.

[16] V. Meshram, P. V. N. Meghana, R. Sahana, L. S. Lasya, and S. S. Reddy, "IoT-Based Alert System for Geriatric," Manipal Journal of Science and Technology, vol. 7, no. 2, article no. 2, 2022.

[17] Y. Tian, Z. Zhang, L. Tian, and W. Zhao, "Design and Research of Indoor Lighting Control System Based on the STM32," International Journal of Advanced Network, Monitoring and Controls, vol. 07, no. 03, pp. 33-42, 2022.

[18] H. S. Sahu, N. Himanish, K. K. Hiran, and J. Leha, "Design of Automatic Lighting System Based on Intensity of Sunlight Using BH-1750," International Conference on Computing, Communication and Green Engineering, pp. 1-6, 2021.

[19] R. T. Yunardi, A. A. Firdaus, M. N. Abdulloh, S. D. N. Nahdliyah, and K. T. Putra, "Relay Module IoT Devices for Remote Controlling of Home Automation System," 2nd International Conference on Electronic and Electrical Engineering and Intelligent System, pp. 350-354, 2022.

[20] W.O. Adedeji and T. S. Amosun, "Design of a PLC Based Temperature Controlled System," R.E.M. (Rekayasa Energi Manufaktur) Jurnal, vol. 8, no. 2, pp. 93-100, 2023.

[21] S. F. Perdana, "AC 220V Digital Thermostat Based Drying Oven Xh-W3001 to Improve Temperature Accuracy in the Drying Process of Black Betel Leaves (Piper betle var Nigra) at Pt. Fbion Karanganyar," 2nd International Conference on Early Childhood Education in Multiperspective, vol. 2, pp. 395-406, 2023.